Effect of collective enhancement in level density in the fission of pre-actinides

Tathagata Banerjee,[1,*] S. Nath,[1] A. Jhingan,[1] N. Saneesh,[1] Mohit Kumar,[1] Abhishek Yadav,[1] Gurpreet Kaur,[2] R. Dubey,[1] M. Shareef,[3] P. V. Laveen,[3] A. Shamlath,[3] Md. Moin Shaikh,[1] S. Biswas,[4] J. Gehlot,[1] K. S. Golda,[1] P. Sugathan,[1] and Santanu Pal[1]

[1]*Nuclear Physics Group, Inter University Accelerator Centre, Aruna Asaf Ali Marg, Post Box 10502, New Delhi 110067, India*

[2]*Department of Physics, Panjab University, Chandigarh 160014, India*

[3]*Department of Physics, School of Mathematical and Physical Sciences, Central University of Kerala, Kasaragod 671314, India*

[4]*Department of Physics, Murshidabad College of Engineering and Technology, Cossimbazar Raj, Berhampore, Murshidabad 742102, India*

(Received 23 May 2017; published 27 July 2017)

Fission fragment angular distributions for three reactions, $^{19}F + ^{182}W$, $^{19}F + ^{187}Re$, and $^{19}F + ^{193}Ir$, are measured in the laboratory energy range of 82–120 MeV. Extracted fission cross sections of the present systems as well as those of three others from literature ($^{19}F + ^{192}Os$, $^{19}F + ^{194}Pt$, and $^{19}F + ^{197}Au$) are compared with the predictions of a statistical model which takes into account the effects of shell, orientation degree of freedom, and collective enhancement in level density (CELD). In all the cases, the standard statistical model predictions overestimate the measured fission cross section, indicating the presence of some amount of dynamical effects in the exit channel. A dissipation strength of 2×10^{21} s^{-1} is found to be sufficient to reproduce the data of all the reactions. No scaling of fission barrier height to fit the data is required.

DOI: 10.1103/PhysRevC.96.014618

I. INTRODUCTION

The fission cross section of heavy-ion-induced fusion reactions, leading to compound nuclei (CN) in the pre-actinide region, is the outcome of competing decay mechanisms of fission and (mostly) neutron evaporation and hence is a sensitive tool for studying the fission process. A reduction in fission barrier height, or fission enhancement, is usually required in the standard statistical model (SM) calculations in order to reproduce the experimental fission (σ_{fis}) or evaporation residue (ER) (σ_{ER}) cross sections [1–7]. This, however, is in contrast with the fission hindrance found necessary to explain the multiplicity of prescission neutrons (ν_{pre}) in similar reactions [8–14]. This clearly calls for further experimental and theoretical investigations.

In the present work, we investigate the de-excitation of six pre-actinide CN, viz., $^{201}_{83}Bi$, $^{206}_{84}Po$, $^{211}_{85}At$, $^{212}_{86}Rn$, $^{213}_{87}Fr$, and $^{216}_{88}Ra$ formed by ^{19}F-induced reactions. Fission fragment (FF) angular distributions and σ_{fis} of the three reactions ($^{19}F + ^{182}W$, $^{19}F + ^{187}Re$, and $^{19}F + ^{193}Ir$ forming the CN $^{201}_{83}Bi$, $^{206}_{84}Po$, and $^{212}_{86}Rn$, respectively) are measured presently. The σ_{fis} of the other three reactions ($^{19}F + ^{192}Os$, $^{19}F + ^{194}Pt$, and $^{19}F + ^{197}Au$ forming the CN $^{211}_{85}At$, $^{213}_{87}Fr$, and $^{216}_{88}Ra$, respectively) are taken from the literature [15–20] and included here for analysis.

II. EXPERIMENTAL DETAILS

A ^{19}F beam, in the laboratory energy (E_{lab}) range of 82–120 MeV, from the 15UD Pelletron accelerator of IUAC, New Delhi, is bombarded onto three isotopically enriched targets ^{182}W (70 μg/cm^2), ^{187}Re (60 μg/cm^2), and ^{193}Ir (80 μg/cm^2) with $\sim$25 μg/cm^2 thick ^{nat}C backing. FFs are detected by nine hybrid telescope (E-ΔE) detectors [21], mounted on the rotatable arms of the general purpose scattering chamber (GPSC), with large angular coverage $\theta_{lab} = 41$–170°. Each telescope consists of an ionization chamber (IC) followed by a silicon detector (E). The isobutane gas pressure at each ΔE is kept at 68 mbar. Two passivated implanted planar silicon detectors are mounted at a laboratory angle (θ_{lab}) of 10° with respect to the beam direction, in the horizontal plane, for monitoring the beam and absolute normalization of cross sections. The schematic of the experimental set up and other details can be found elsewhere [22].

III. RESULTS

FFs are unambiguously distinguished from the other reaction products based on energy loss and residual energy. Measured angular distributions are transformed to the center-of-mass (c.m.) frame of reference by assuming symmetric mass division and using the Viola systematics [23] for FF kinetic energies. The FF angular distributions in the c.m. frame of reference, $\frac{d\sigma_{fis}}{d\Omega}(\theta_{c.m.})$ thus obtained, are fitted by the exact theoretical expression for the angular distribution function [$W(\theta_{c.m.})$] as described in Ref. [22]. Figure 1 shows the experimental FF angular distributions along with the fitted curves for $^{19}F + ^{182}W$. Experimental angular anisotropy (A_{exp}) is obtained from the ratio $\frac{W(180^\circ)}{W(90^\circ)}$.

The reliability of the capture ℓ distribution used in our subsequent analysis is verified by reproducing the experimental capture excitation functions of $^{19}F + ^{182}W$, $^{19}F + ^{192}Os$, $^{19}F + ^{194}Pt$, and $^{19}F + ^{197}Au$ reactions (Fig. 2). The data are fitted by the coupled-channels code CCFULL [25]. The deformation parameters used in coupled-channels calculation are taken from standard tables [26–28]. For each odd-mass target, deformation parameters and energy of the first 2^+ excited state are approximated by averaging the corresponding values in neighboring even-even nuclei. The low-lying inelastic states of ^{19}F are also included in the calculation. Potential parameters, i.e., depth `V0`, radius `r0`, and diffuseness `a`, are obtained

*he.tatha@gmail.com

 ©2017 American Physical Society

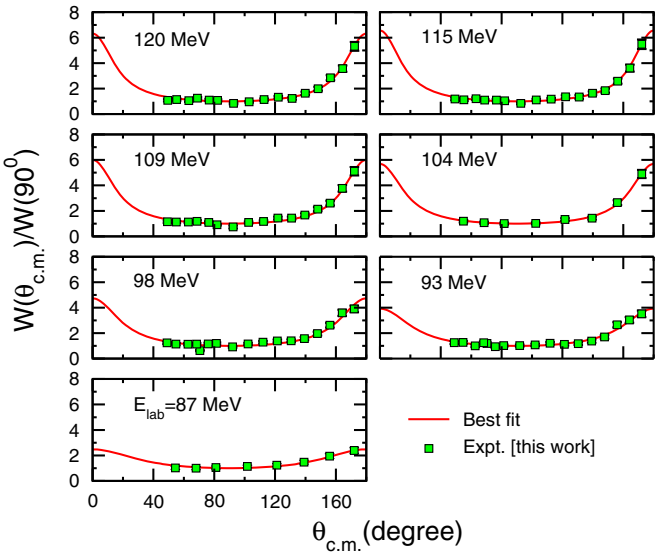

FIG. 1. Measured fission fragment angular distributions along with the best fit to data for the reaction $^{19}\mathrm{F} + {}^{182}\mathrm{W}$.

from the Woods-Saxon parametrization of the Akyüz-Winther potential. In some cases, a deeper potential well (by about 10% of the original value) are required to reproduce the experimental capture cross sections (σ_{cap}).

Theoretical fission angular anisotropies are obtained from the statistical saddle-point model (SSPM) [29],

$$A_{\mathrm{cal}} \approx 1 + \frac{\langle J^2 \rangle}{4K_0^2}, \tag{1}$$

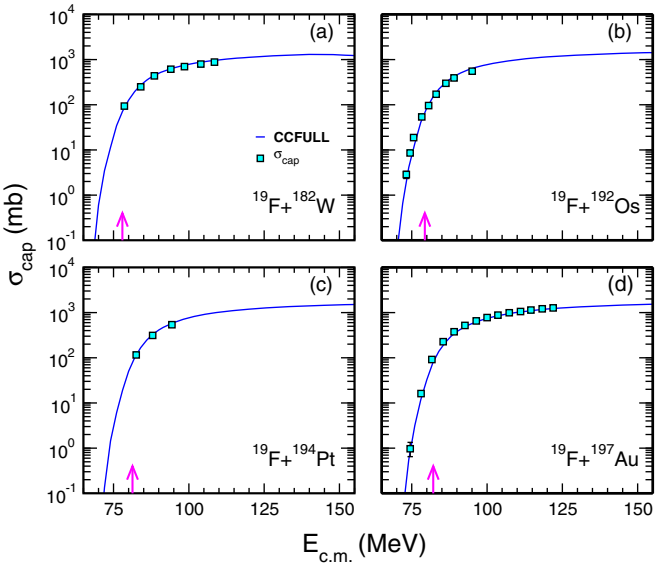

FIG. 2. Experimental (square box) and theoretical σ_{cap} for (a) $^{19}\mathrm{F} + {}^{182}\mathrm{W}$, (b) $^{19}\mathrm{F} + {}^{192}\mathrm{Os}$, (c) $^{19}\mathrm{F} + {}^{194}\mathrm{Pt}$, and (d) $^{19}\mathrm{F} + {}^{197}\mathrm{Au}$ reactions. The vertical arrow in each panel indicates position of the Coulomb barrier. Experimental data for the different systems are taken from (a) fission from present study plus ER from Ref. [24], (b) from Ref. [15], (c) from Ref. [16], and (d) from Ref. [19].

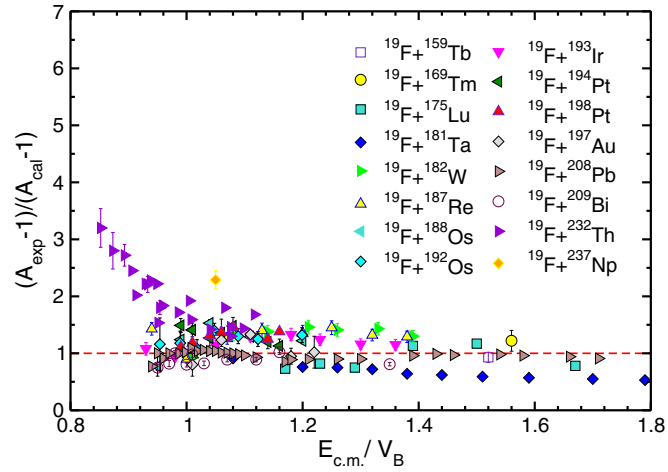

FIG. 3. $\frac{A_{\mathrm{exp}}-1}{A_{\mathrm{cal}}-1}$ as a function of $\frac{E_{\mathrm{c.m.}}}{V_{\mathrm{B}}}$ for reactions involving $^{19}\mathrm{F}$ projectile on various targets. Here V_{B} is the Coulomb barrier. Data for the systems other than the present one are obtained from the literature (see text).

where K_0 is given by

$$K_0^2 = \frac{\mathcal{I}_{\mathrm{eff}}}{\hbar^2} T_{\mathrm{sad}}, \tag{2}$$

and $\mathcal{I}_{\mathrm{eff}}$ is the effective moment of inertia at the saddle point. The saddle-point temperature is calculated from the expression

$$T_{\mathrm{sad}} = \left[\frac{E_{\mathrm{c.m.}} + Q - B_{\mathrm{f}}^{\mathrm{LDM}}(\ell) - E_{\mathrm{rot}}(\ell) - E_{\mathrm{n}}}{a} \right]^{\frac{1}{2}}, \tag{3}$$

where $E_{\mathrm{c.m.}}$ is the incident energy in the center-of-mass (c.m.) frame of reference and Q is the Q value for formation of the CN. $B_{\mathrm{f}}^{\mathrm{LDM}}(\ell)$ and $E_{\mathrm{rot}}(\ell)$ are the ℓ-dependent fission barrier and rotational energy, respectively. E_{n} is the average energy removed by the evaporated neutrons from the CN. $\mathcal{I}_{\mathrm{eff}}$, $B_{\mathrm{f}}^{\mathrm{LDM}}(\ell)$ and $E_{\mathrm{rot}}(\ell)$ are calculated by the rotating finite-range model (RFRM) of Sierk [30] while evaluating A_{cal}. E_{n} is obtained from the systematics of Itkis *et al.* [31]. Mean of the square of total angular momentum of the fissioning nucleus, $\langle J^2 \rangle$, is calculated by the SM code PACE3 [32] in traceback mode. The level density parameter (a) is taken as $\frac{A}{9}$ up to $^{19}\mathrm{F} + {}^{198}\mathrm{Pt}$. For the remaining heavier systems, $a = \frac{A}{10}$ is employed in the PACE3 calculation.

Both the ratio of a at the saddle point to that in the ground state ($\frac{a_{\mathrm{f}}}{a_{\mathrm{n}}}$) and the scaling factor for the RFRM fission barrier (k_{f}) are taken as unity in the present analysis.

In order to compare the experimental and theoretical angular anisotropies, the ratio $\frac{A_{\mathrm{exp}}-1}{A_{\mathrm{cal}}-1}$ is plotted for the measured systems as well as thirteen more ^{19}F-induced reactions, data for which are taken from literature [15,16,20,33–43], in Fig. 3. Departure of $\frac{A_{\mathrm{exp}}-1}{A_{\mathrm{cal}}-1}$ from unity is subdued for systems with targets having large ground-state spin, e.g., $^{175}\mathrm{Lu}(\frac{7}{2}^+)$ and $^{181}\mathrm{Ta}$ $(\frac{7}{2}^+)$, as was already mentioned in Ref. [22]. Otherwise, deviation of the above ratio from unity for targets with zero ground-state spin indicates presence of noncompound nuclear fission (NCNF). Though NCNF can be present in pre-actinide

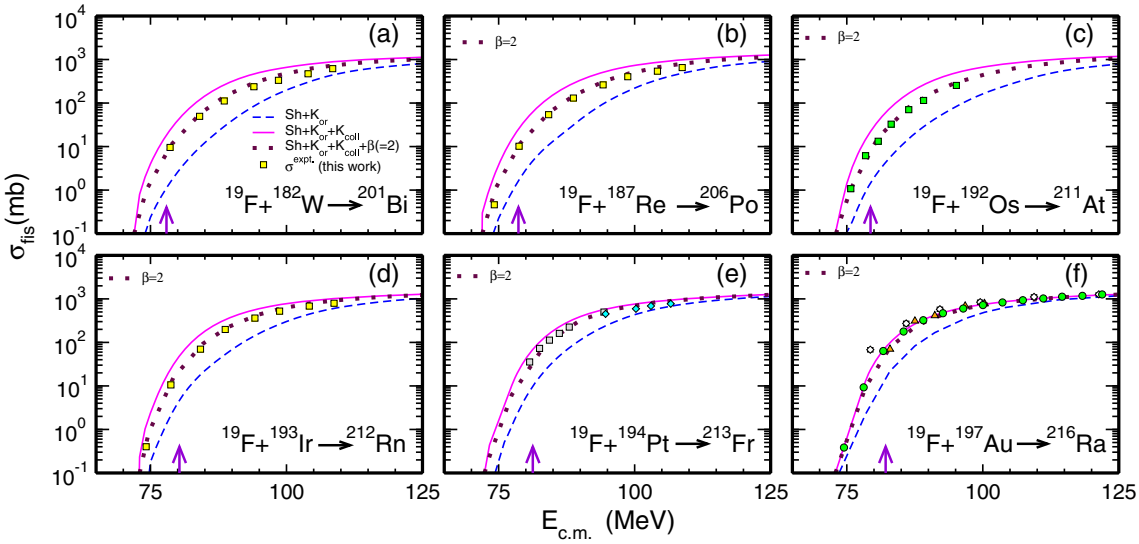

FIG. 4. Measured and calculated $\sigma_{\rm fis}$ for (a) ^{19}F + ^{182}W, (b) ^{19}F + ^{187}Re, (c) ^{19}F + ^{192}Os, (d) ^{19}F + ^{193}Ir, (e) ^{19}F + ^{194}Pt, and (f) ^{19}F + ^{197}Au. Data points from the present work are shown with solid yellow squares. Data for the systems other than the present ones: Solid green squares in panel (c) are from Ref. [15], solid gray squares and solid cyan diamonds in panel (e) from Refs. [16] and [17], respectively, and hollow diamonds, solid green circles, and solid orange triangles in panel (f) are from Refs. [18], [19] and [20], respectively. The dashed blue lines are the predictions including only shell (Sh) and K-orientation ($K_{\rm or}$) effects. The continuous magenta lines represent VECSTAT predictions including the effects of shell, K orientation, and CELD ($K_{\rm coll}$). The dotted maroon lines represent VECSTAT predictions including the effects of shell, K orientation, CELD, and a suitable strength of dissipation. The vertical arrow in each panel indicates position of the Coulomb barrier.

CN populated by heavier projectiles (e.g., ^{28}Si) [22,44], the present study of FF anisotropies of ^{19}F-induced reactions (Fig. 3) shows that no prominent signature of the presence of NCNF appears until one enters into the actinide region. One can therefore assume that all capture events in the current six systems lead to CN formation and hence can be subjected to SM analysis of CN decay.

The experimental $\sigma_{\rm fis}$ for the three reactions are obtained by integrating the measured $\frac{d\sigma_{\rm fis}}{d\Omega}(\theta_{\rm c.m.})$. Measured fission excitation functions are shown in Fig. 4 and the cross sections are listed in Table I.

The experimental $\sigma_{\rm fis}$ are next compared with the statistical model predictions. The CN can decay into two major products, namely an evaporation residue (ER) or the FFs, along with the emission of light particles like neutrons, protons, α particles, and γ rays. In the SM calculation, the particle and γ emission widths are obtained from the Weisskopf formula as given in Ref. [45] and the fission width is obtained from the transition-state model due to Bohr and Wheeler [46]. The fission barrier in the present calculation is obtained by including shell correction in the liquid-drop nuclear mass [47]. The shell correction term δ is given as the difference between the experimental and the liquid-drop model (LDM) masses, ($\delta = M_{\rm exp} - M_{\rm LDM}$) [48]. The fission barrier then is given as

$$B_{\rm f}(\ell) = B_{\rm f}^{\rm LDM}(\ell) - (\delta_{\rm g} - \delta_{\rm s}) \qquad (4)$$

where $B_{\rm f}^{\rm LDM}(\ell)$ is the angular-momentum-dependent LDM fission barrier obtained from [30] and $\delta_{\rm g}$ and $\delta_{\rm s}$ are the shell correction energies for the ground-state and saddle configurations respectively. $\delta_{\rm g}$ and $\delta_{\rm s}$ are obtained from Ref. [49], which gives a prescription for deformation-dependent shell correction and gives a very small value of shell correction at large deformations and full shell correction at zero deformation. Shell effect is also included in the nuclear level density which

TABLE I. Measured fission cross sections and fission angular anisotropies. Energy in the center-of-mass frame of reference ($E_{\rm c.m.}$) and the excitation energy (E^*) are given at the center of the target.

CN	$E_{\rm c.m.}$ (MeV)	E^* (MeV)	$\sigma_{\rm fis}$ (mb)	$A_{\rm exp}$
$^{201}_{83}$Bi$_{118}$	78.6	50.3	9.6 ± 1.0	2.47 ± 0.25
	84.0	55.7	49.6 ± 5.0	3.92 ± 0.39
	88.6	60.2	111.6 ± 11.2	4.73 ± 0.38
	94.0	65.7	237.4 ± 23.7	5.68 ± 0.57
	98.5	70.2	333.6 ± 33.4	6.00 ± 0.60
	104.0	75.6	471.4 ± 47.1	6.55 ± 0.66
	108.5	80.2	617.5 ± 61.8	6.32 ± 0.63
$^{206}_{84}$Po$_{122}$	74.2	49.7	0.46 ± 0.05	2.33 ± 0.19
	78.8	54.2	10.2 ± 1.0	2.26 ± 0.23
	84.2	59.7	54.0 ± 5.4	3.45 ± 0.34
	88.7	64.2	130.2 ± 13.0	4.38 ± 0.35
	94.2	69.7	261.3 ± 26.1	5.20 ± 0.42
	98.7	74.2	403.3 ± 40.3	5.87 ± 0.59
	104.2	79.7	538.9 ± 53.9	5.70 ± 0.57
	108.7	84.2	653.9 ± 65.4	5.93 ± 0.59
$^{212}_{86}$Rn$_{126}$	74.4	47.0	0.40 ± 0.04	1.67 ± 0.17
	79.0	51.6	10.6 ± 1.1	1.75 ± 0.17
	84.4	57.1	69.9 ± 7.0	2.43 ± 0.24
	89.0	61.6	198.0 ± 19.8	3.12 ± 0.31
	94.4	67.1	362.1 ± 36.2	3.80 ± 0.38
	99.0	71.6	523.2 ± 52.3	4.01 ± 0.40
	104.5	77.1	683.9 ± 68.4	4.28 ± 0.43
	109.0	81.7	794.1 ± 79.4	4.61 ± 0.46

is used to calculate various decay widths of the CN. We use the level density parameter from the work of Ignatyuk *et al.* [50], which includes shell effects at low excitation energies and goes over to its asymptotic form at high excitation energies. The shape-dependent asymptotic level density is taken from Ref. [51].

We next include the effect of K-degree (CN spin component along the symmetry axis) of freedom in fission width. The angular momentum of a CN can tilt away from its initial direction, perpendicular to the symmetry axis ($K = 0$), to nonzero values of K due to the coupling of the K degree of freedom with intrinsic nuclear motion [52]. Assuming a fast equilibration of the K degree of freedom, the fission width is given as [53]

$$\Gamma_f(E^*,J)=\Gamma_f(E^*,J,K=0)\frac{(K_0\sqrt{2\pi})}{2J+1}\,\mathrm{erf}\left(\frac{J+1/2}{K_0\sqrt{2}}\right) \quad (5)$$

with $K_0^2 = \frac{\tau_{\rm eff}}{\hbar^2}T_{\rm sad}$, where $\tau_{\rm eff}$ is the effective moment of inertia ($\frac{1}{\tau_{\rm eff}}=\frac{1}{\tau_\parallel}-\frac{1}{\tau_\perp}$) and $\tau_\perp$ and $\tau_\parallel$ are the moments of inertia at saddle of the nucleus perpendicular to and about the nuclear symmetry axis. erf(x) is the error function. $\Gamma_f(E^*,J,K=0)$ represents the Bohr-Wheeler fission width [46].

Incorporating the above-mentioned shell effects in fission barrier and level density and the K-orientation effect in the statistical model code VECSTAT [54], fission excitation functions are obtained for all the six systems and are compared with the experimental values in Fig. 4. Evidently, the statistical model (dashed blue line) underestimates the fission cross sections.

It was shown earlier by Bjørnholm *et al.* [55] that the collective motion in a nucleus gives rise to an enhancement of nuclear level density with respect to the intrinsic level density, $\rho_{\rm intr}(E^*)$ and is given as $\rho(E^*) = K_{\rm coll}(E^*)\rho_{\rm intr}(E^*)$, where $\rho(E^*)$ is the total level density and $K_{\rm coll}$ is the enhancement factor. The effect of CELD is included in the present calculation following the work of Zagrebaev *et al.* [56], where the enhancement changes from vibrational ($K_{\rm vib}$) to rotational ($K_{\rm rot}$) type with increasing quadrupole deformation β_2 of a nucleus. The transition is implemented through a function $\varphi(\beta_2)$ as follows:

$$K_{\rm coll}(\beta_2) = \{K_{\rm rot}\varphi(\beta_2) + K_{\rm vib}[1-\varphi(\beta_2)]\}\, f(E^*), \quad (6)$$

where

$$\varphi(\beta_2) = \left[1+\exp\left(\frac{\beta_2^0-\beta_2}{\Delta\beta_2}\right)\right]^{-1}. \quad (7)$$

The values of $\beta_2^0 = 0.15$ and $\Delta\beta_2 = 0.04$ are taken from Ref. [57]. The Fermi function $f(E^*)$ represents the damping of collectivity with increasing excitation enegy E^* and is given as

$$f(E^*) = \left[1+\exp\left(\frac{E^*-E_{\rm cr}}{\Delta E}\right)\right]^{-1} \quad (8)$$

with $E_{\rm cr} = 40$ MeV and $\Delta E = 10$ MeV [58]. The rotational and vibrational enhancement factors are given as $K_{\rm rot} = \frac{\tau_\perp T}{\hbar^2}$ and $K_{\rm vib} = e^{0.055\times A^{\frac{2}{3}}\times T^{\frac{4}{3}}}$, where A is the nuclear mass number, T is the nuclear temperature, and $\tau_\perp$ is the rigid-body moment of inertia perpendicular to the symmetry axis [59]. By definition of CELD, the lower limit of $K_{\rm coll}$ is set as unity. CELD is applied to the level densities of both the parent and the daughter nuclei in calculations of the widths of various evaporation channels. CELD is also included in the level densities at both the ground state and at the saddle in fission width calculation. CELD at ground state is calculated using experimental values of β_2 for deformed nuclei.

The effect of CELD on calculated fission excitation functions is also shown in Fig. 4 (continuous magenta lines). It is observed that CELD increases $\sigma_{\rm fis}$ substantially for all the systems except ^{19}F + ^{194}Pt and ^{19}F + ^{197}Au. The last two systems are highly fissile and $\sigma_{\rm fis}$ for them account for almost the entire $\sigma_{\rm cap}$. This leaves no room for further increase of $\sigma_{\rm fis}$ even if the fission widths increase due to CELD. The strong enhancement of fission width due to CELD can be understood as follows. With the saddle shape being highly deformed, the level density enhancement factor at saddle is of rotational type while it is of vibrational nature for spherical nuclei at ground state. The typical values of $K_{\rm vib}$ are ∼1–10, while those of $K_{\rm rot}$ lie in the range ∼100–150. Since the transition-state fission width is given by the ratio of the number of levels available at the saddle to those at the ground state, CELD can significantly increase the fission width for spherical nuclei. This is reflected in SM results given in Fig. 4 for the present systems for which the CN are spherical at ground state and thus an increase of $\sigma_{\rm fis}$ is observed. It may, however, be noted that for nuclei with strong ground-state deformation, the enhancement factors at both the saddle and the ground state are of rotational type with similar magnitudes, resulting in a marginal effect on the fission width.

The observation in Fig. 4 that the calculated $\sigma_{\rm fis}$ are larger than the experimental values suggests that hindrance in fission is to be taken into consideration. In a dissipative dynamical model of fission, a reduction in fission width is obtained from the Kramers-modified fission width and is given as [60]

$$\Gamma_K = \Gamma_f\left\{\sqrt{1+\left(\frac{\beta}{2\omega_s}\right)^2}-\frac{\beta}{2\omega_s}\right\} \quad (9)$$

where β is the reduced dissipation coefficient (ratio of dissipation coefficient to inertia) and ω_s is the local frequency of a harmonic oscillator potential which approximates the nuclear potential at the saddle configuration and depends on the spin of the CN [61]. Γ_f is the Bohr-Wheeler fission width obtained with shell-corrected level densities, CELD, and K-orientation effect. For the CN studied here, a value of $\beta = 2\times10^{21}$ s^{-1} (dotted maroon lines in Fig. 4) is required to reproduce $\sigma_{\rm fis}$. It may, however, be pointed out that $\sigma_{\rm fis}$ for the two most asymmetric reactions leading to CN ^{213}Fr and ^{216}Ra are not sensitive to the strength of β due to their high fissility, as has been discussed in a preceding paragraph.

The effect of CELD in nuclear decay was examined earlier by various authors [56,58,59,62,63]. Junghans *et al.* [58] found a significant role of CELD in reproducing the mass distribution from fragmentation of heavy nuclei. The lack of stabilizing influence of shell closure on the survival probability of CN with $N = 126$ has been noted earlier and has been attributed

to the enhanced fission probability due to CELD [58,64,65]. Mayorov *et al.* [66] showed that inclusion of CELD gives better agreement with experimental σ_{ER} for CN near $N = 126$. Incorporation of CELD was also found to be important for predicting the survival property of superheavy nuclei [67]. Evidence of CELD has also been found in the evaporation neutron spectrum from deformed CN [63].

On the other hand, it was observed that α-particle spectrum could not be reproduced when CELD was considered [68]. Siwek-Wilczynska *et al.* [69] did not find it necessary to consider any additional factor such as CELD or Kramers hindrance factor to reproduce σ_{ER} at low excitation energies. Sagaidak *et al.* [5] also concluded against considering CELD in order to explain de-excitation of different isotopes of Po, formed in heavy-ion-induced fusion reactions.

IV. CONCLUSIONS

In the present work, we find that inclusion of CELD along with the shell and K-orientation effects in SM analysis gives a consistent picture of fission cross sections in the pre-actinide region populated by ^{19}F projectile where a fission hindrance is required as is also the case for explaining prescission neutron multiplicity. With the strength of dissipation as the only adjustable parameter in the present SM calculation, it is observed that an energy-independent strength of the reduced dissipation coefficient ($\beta = 2 \times 10^{21}$ s^{-1}) can reproduce the experimental fission excitation functions of all the systems considered here.

ACKNOWLEDGMENTS

The authors thank Jhilam Sadhukhan of VECC, Kolkata, for providing the form factor of deformation-dependent shell correction. One of the authors (T.B.) acknowledges the University Grants Commission (UGC), Government of India, for financial support. M.S. acknowledges Kerala State Council for Science, Technology, and Environment (KSCSTE) for financial support in the form of a fellowship.

[1] K.-T. Brinkmann, A. L. Caraley, B. J. Fineman, N. Gan, J. Velkovska, and R. L. McGrath, Phys. Rev. C **50**, 309 (1994).
[2] A. N. Andreyev, D. D. Bogdanov, V. I. Chepigin, A. P. Kabachenko, O. N. Malyshev, Y. T. Oganessian, A. G. Popeko, J. Rohác, R. N. Sagaidak, G. M. Ter-Akopian *et al.*, Nucl. Phys. A **626**, 857 (1997).
[3] R. N. Sagaidak, G. N. Kniajeva, I. M. Itkis, M. G. Itkis, N. A. Kondratiev, E. M. Kozulin, I. V. Pokrovsky, A. I. Svirikhin, V. M. Voskressensky, A. V. Yeremin *et al.*, Phys. Rev. C **68**, 014603 (2003).
[4] L. Corradi, B. R. Behera, E. Fioretto, A. Gadea, A. Latina, A. M. Stefanini, S. Szilner, M. Trotta, Y. Wu, S. Beghini *et al.*, Phys. Rev. C **71**, 014609 (2005).
[5] R. N. Sagaidak and A. N. Andreyev, Phys. Rev. C **79**, 054613 (2009).
[6] S. Nath, P. V. M. Rao, S. Pal, J. Gehlot, E. Prasad, G. Mohanto, S. Kalkal, J. Sadhukhan, P. D. Shidling, K. S. Golda *et al.*, Phys. Rev. C **81**, 064601 (2010).
[7] V. Singh, B. R. Behera, M. Kaur, A. Kumar, K. P. Singh, N. Madhavan, S. Nath, J. Gehlot, G. Mohanto, A. Jhingan *et al.*, Phys. Rev. C **89**, 024609 (2014).
[8] D. J. Hinde, R. J. Charity, G. S. Foote, J. R. Leigh, J. O. Newton, S. Ogaza, and A. Chattejee, Nucl. Phys. A **452**, 550 (1986).
[9] J. O. Newton, D. J. Hinde, R. J. Charity, J. R. Leigh, J. J. M. Bokhorst, A. Chatterjee, G. S. Foote, and S. Ogaza, Nucl. Phys. A **483**, 126 (1988).
[10] H. Singh, A. Kumar, B. R. Behera, I. M. Govil, K. S. Golda, P. Kumar, A. Jhingan, R. P. Singh, P. Sugathan, M. B. Chatterjee, S. K. Datta, Ranjeet, S. Pal, and G. Viesti, Phys. Rev. C **76**, 044610 (2007).
[11] H. Singh, K. S. Golda, S. Pal, Ranjeet, R. Sandal, B. R. Behera, G. Singh, A. Jhingan, R. P. Singh, P. Sugathan, M. B. Chatterjee, S. K. Datta, A. Kumar, G. Viesti, and I. M. Govil, Phys. Rev. C **78**, 024609 (2008).
[12] V. Singh, B. R. Behera, M. Kaur, A. Kumar, P. Sugathan, K. S. Golda, A. Jhingan, M. B. Chatterjee, R. K. Bhowmik, D. Siwal *et al.*, Phys. Rev. C **87**, 064601 (2013).
[13] R. Sandal *et al.*, Phys. Rev. C **87**, 014604 (2013).
[14] I. Mukul, S. Nath, K. S. Golda, A. Jhingan, J. Gehlot, E. Prasad, S. Kalkal, M. B. Naik, T. Banerjee, T. Varughese *et al.*, Phys. Rev. C **92**, 054606 (2015).
[15] K. Mahata *et al.*, Nucl. Phys. A **720**, 209 (2003).
[16] K. Mahata, S. Kailas, A. Shrivastava, A. Chatterjee, P. Singh, S. Santra, and B. S. Tomar, Phys. Rev. C **65**, 034613 (2002).
[17] V. Singh *et al.*, EPJ Web Conf. **86**, 00052 (2015).
[18] H. Ikezoe, N. Shikazono, Y. Nagame, Y. Sugiyama, Y. Tomita, K. Ideno, A. Iwamoto, and T. Ohtsuki, Phys. Rev. C **42**, 342 (1990).
[19] D. J. Hinde, A. C. Berriman, R. D. Butt, M. Dasgupta, I. I. Gontchar, C. R. Morton, A. Mukherjee, and J. O. Newton, J. Nucl. Radiochem. Sci. **3**, 31 (2002).
[20] R. Tripathi, K. Sudarshan, S. Sodaye, A. V. R. Reddy, K. Mahata, and A. Goswami, Phys. Rev. C **71**, 044616 (2005).
[21] A. Jhingan, G. Kaur, N. Saneesh, T. Banerjee, R. Ahuja, B. R. Behera, and P. Sugathan, *Proceedings of the DAE Symposium on Nuclear Physics*, Vol. 59 (Board of Research in Nuclear Science, Mumbai, 2014), p. 830.
[22] T. Banerjee *et al.*, Phys. Rev. C **94**, 044607 (2016).
[23] V. E. Viola, K. Kwiatkowski, and M. Walker, Phys. Rev. C **31**, 1550 (1985).
[24] J. Gehlot *et al.*, *Proceedings of the DAE-BRNS Symposium on Nuclear Physics*, Vol. 61 (Board of Research in Nuclear Science, Mumbai, 2016), p. 404.
[25] K. Hagino, N. Rowley, and A. T. Kruppa, Comput. Phys. Commun. **123**, 143 (1999).
[26] R. H. Spear, Phys. Rep. **73**, 369 (1981).
[27] P. Moller, J. R. Nix, W. D. Myers, and W. J. Swiatecki, At. Data Nucl. Data Tables **59**, 185 (1995).
[28] http://www.nndc.bnl.gov/
[29] I. Halpern and V. M. Strutinsky, Proc. Int. Conf. Peaceful Uses of Atomic Energy, Geneva, **15**, 408 (1958).
[30] A. J. Sierk, Phys. Rev. C **33**, 2039 (1986).
[31] M. G. Itkis and A. Y. Rusanov, Phys. Part. Nuclei **29**, 160 (1998).
[32] A. Gavron, Phys. Rev. C **21**, 230 (1980).
[33] R. J. Charity *et al.*, Nucl. Phys. A **457**, 441 (1986).

[34] A. Chatterjee *et al.*, *Proceedings of the DAE Symposium on Nuclear Physics*, Vol. 39B (Board of Research in Nuclear Science, Mumbai, 1996), p. 170.
[35] H. Ikezoe, N. Shikazono, Y. Nagame, Y. Sugiyama, Y. Tomita, K. Ideno, I. Nishinaka, B. J. Qi, H. J. Kim, A. Iwamoto, and T. Ohtsuki, Phys. Rev. C **46**, 1922 (1992).
[36] B. Qi *et al.*, JAERI Lab Report JAERI-M-91-188, 1991, http://www.iaea.org/inis/collection/NCLCollectionStore/_Public/23/023/23023935.pdf.
[37] D. J. Hinde, A. C. Berriman, M. Dasgupta, J. R. Leigh, J. C. Mein, C. R. Morton, and J. O. Newton, Phys. Rev. C **60**, 054602 (1999).
[38] A. M. Samant, S. Kailas, A. Chatterjee, A. Shrivastava, A. Navin, and P. Singh, Eur. Phys. J. A **7**, 59 (2000).
[39] H. Fujiwara, S. C. Jeong, Y. H. Pu, T. Mizota, H. Kugoh, Y. Futami, Y. Nagashima, and S. M. Lee, Annual Report of University of Tsukuba (Japan), Report No. UTTAC-57, p. 52 (1989) (unpublished), https://inis.iaea.org/search/search.aspx?orig_q=reportnumber:%22UTTAC–57%22.
[40] S. Kailas, A. Navin, A. Chatterjee, P. Singh, R. K. Choudhury, A. Saxena, D. M. Nadkarni, S. S. Kapoor, V. S. Ramamurthy, B. K. Nayak, and S. V. Suryanarayana, Phys. Rev. C **43**, 1466 (1991).
[41] H. Zhang *et al.*, Phys. Rev. C **49**, 926 (1994).
[42] N. Majumdar, P. Bhattacharya, D. C. Biswas, R. K. Choudhury, D. M. Nadkarni, and A. Saxena, Phys. Rev. C **51**, 3109 (1995).
[43] V. S. Ramamurthy, S. S. Kapoor, R. K. Choudhury, A. Saxena, D. M. Nadkarni, A. K. Mohanty, B. K. Nayak, S. V. Sastry, S. Kailas, A. Chatterjee *et al.*, Phys. Rev. Lett. **65**, 25 (1990).
[44] T. Banerjee, S. Nath, and S. Pal, Phys. Rev. C **91**, 034619 (2015).
[45] P. Fröbrich and I. I. Gontchar, Phys. Rep. **292**, 131 (1998).
[46] N. Bohr and J. A. Wheeler, Phys. Rev. **56**, 426 (1939).
[47] K. Mahata, S. Kailas, and S. S. Kapoor, Phys. Rev. C **92**, 034602 (2015).
[48] W. D. Myers and W. J. Swiatecki, Report No. LBL-36803, Lawrence Berkeley National Laboratory, Berkeley, California, 1994 (unpublished).
[49] W. D. Myers and W. J. Swiatecki, Nucl. Phys. **81**, 1 (1966).
[50] A. V. Ignatyuk, M. G. Itkis, V. N. Okolovich, G. M. Smirenkin, and A. Tishin, Yad. Fiz. **21**, 485 (1975) Sov. J. Nucl. Phys. **21**, 255 (1975).
[51] W. Reisdorf, Z. Phys. A **300**, 227 (1981).
[52] J. P. Lestone and S. G. McCalla, Phys. Rev. C **79**, 044611 (2009).
[53] J. P. Lestone, Phys. Rev. C **59**, 1540 (1999).
[54] J. Sadhukhan, Ph.D. thesis, Homi Bhabha National Institute, Mumbai, 2012.
[55] S. Bjørnholm, A. Bohr, and B. R. Mottelson, in *Proceedings of the International Conference on the Physics and Chemistry of Fission, Rochester 1973* (IAEA, Vienna, 1974), Vol. 1, p. 367.
[56] V. I. Zagrebaev, Y. Aritomo, M. G. Itkis, Y. T. Oganessian, and M. Ohta, Phys. Rev. C **65**, 014607 (2001).
[57] M. Ohta, in *Proceedings on Fusion Dynamics at the Extremes, Dubna, 2000*, edited by Y. T. Oganessian and V. I. Zagrebaev (World Scientific, Singapore, 2001), p. 110.
[58] A. R. Junghans, M. de Jong, H.-G. Clerc, A. V. Ignatyuk, G. A. Kudyaev, and K.-H. Schmidt, Nucl. Phys. A **629**, 635 (1998).
[59] A. V. Ignatyuk, G. N. Smirenkin, M. G. Itkis, S. I. Mulgin, and V. N. Okolovivh, Fiz. Elem. Chastits At. Yadra **16**, 709 (1985) [Sov. J. Part. Nuclei **16**, 307 (1985)].
[60] H. A. Kramers, Phys. (Amsterdam, Neth.) **7**, 284 (1940).
[61] J. Sadhukhan and S. Pal, Phys. Rev. C **78**, 011603(R) (2008); **79**, 019901(E) (2009).
[62] A. Heinz *et al.*, Nucl. Phys. A **713**, 3 (2003).
[63] P. Roy, K. Banerjee, M. Gohil, C. Bhattacharya, S. Kundu, T. K. Rana, T. K. Ghosh, G. Mukherjee, R. Pandey, H. Pai *et al.*, Phys. Rev. C **88**, 031601(R) (2013).
[64] D. Vermeulen *et al.*, Z. Phys. A **318**, 157 (1984).
[65] C. C. Sahm *et al.*, Nucl. Phys. A **441**, 316 (1985).
[66] D. A. Mayorov, T. A. Werke, M. C. Alfonso, M. E. Bennett, and C. M. Folden, Phys. Rev. C **90**, 024602 (2014).
[67] R. Yanez, W. Loveland, L. Yao, J. S. Barrett, S. Zhu, B. B. Back, T. L. Khoo, M. Alcorta, and M. Albers, Phys. Rev. Lett. **112**, 152702 (2014).
[68] S. Komarov, R. J. Charity, C. J. Chiara, W. Reviol, D. G. Sarantites, L. G. Sobotka, A. L. Caraley, M. P. Carpenter, and D. Seweryniak, Phys. Rev. C **75**, 064611 (2007).
[69] K. Siwek-Wilczyńska, I. Skwira, and J. Wilczyński, Phys. Rev. C **72**, 034605 (2005).